Received: 16 May 2023 | Revised: 22 October 2023 | Accepted: 25 October 2023

DOI: 10.1111/jace.19541

FINALIST ARTICLE

Journal of American Ceramic Society

Spatial and temporal control of glassy-crystalline domains in optical phase change materials

Chih-Yu Lee[1] | Chuanyu Lian[1,2] | Hongyi Sun[1,2] | Yi-Siou Huang[1,2] | Niloy Acharjee[2] | Ichiro Takeuchi[1,3] | Carlos A. Ríos Ocampo[1,2]

[1]Department of Materials Science and Engineering, University of Maryland, College Park, Maryland, USA

[2]Institute for Research in Electronics and Applied Physics, University of Maryland, College Park, Maryland, USA

[3]Department of Physics, Quantum Materials Center, University of Maryland, College Park, Maryland, USA

Correspondence
Carlos A. Ríos Ocampo, Department of Materials Science and Engineering, University of Maryland, College Park, MD 20742, USA.
Email: riosc@umd.edu

Editor's Choice
The Editor-in-Chief recommends this outstanding article.

Funding information
Division of Electrical, Communications and Cyber Systems, Grant/Award Number: ECCS-2210168; Multidisciplinary University Research Initiative, Grant/Award Number: N00014-17-1-2661; Division of Materials Research, Grant/Award Number: DMR-2329087

Abstract

Chalcogenide phase change materials (PCMs) have become one of the most promising material platforms for the Optics and Photonics community. The unparalleled combination of nonvolatility and large optical property modulation promises devices with low-energy consumption and ultra-compact form factors. At the core of all these applications lies the difficult task of precisely controlling the glassy amorphous and crystalline domains that compose the PCM microstructure and dictate the optical response. A spatially controllable glassy-crystalline domain distribution is desired for intermediate optical response (vs. binary response between fully amorphous and crystalline states), and temporally resolved domains are sought after for repeatable reconfiguration. In this perspective, we briefly review the fundamentals of PCM phase transition in various reconfiguring approaches for optical devices. We discuss each method's underpinning mechanisms, design, advantages, and downsides. Finally, we lay out current challenges and future directions in this field.

KEYWORDS

chalcogenides, optical materials, phase change materials

1 | INTRODUCTION

Since their discovery by Ovshinsky in 1968,[1] chalcogenide phase change materials (PCMs) have been predominantly used in data storage,[2] leveraging the nonvolatile response and distinct electrical and optical properties of their amorphous and crystalline states. However, developments during the last decade have reinvented such materials in applications exploiting their refractive index/permittivity contrast in amplitude or phase modulation in photonic circuits,[3–7] structural color,[8,9,10] metasurfaces,[11,12] optical metamaterials,[13,14] plasmonics,[14,15] etc. This growing interest has also translated into the development of novel PCMs with optimized optical properties, that is, Optical PCMs (O-PCMs).[16] Moreover, shifting from digital applications—resulting from switching between glassy amorphous and crystalline states only, recent works deploy the analog nature of PCMs to increase multi-level

response via intermediate distributions of both phases for gray-scale colors,[8] higher density data storage,[17] tunable optical response,[5] etc. The precise control of glassy-crystalline spatial and temporal distribution is pivotal to having a robust multi-level and reconfigurable operation, respectively. To achieve such distributions, crystallization or amorphization processes require distinct and precise heat stimuli from optical, electrical, or electro-thermal pulses, whose spatial profile can be engineered. The processing-structure-property relations are thus of extreme relevance for PCMs in novel optical applications, relations that remain largely unexplored despite the fact that PCMs have been studied for decades.

In this work, we study the different state-of-the-art mechanisms to control the glassy-crystalline microstructure of PCMs in a variety of devices and for different applications. Moreover, we discuss our perspectives on potential strategies moving forward. We focus on optical readout only, which, compared to electrical signal readout from resistance change, provides more degrees of freedom; namely, phase, amplitude, mode, polarization, wavelength, etc. Furthermore, the ultrafast light propagation and "unlimited" bandwidth guarantee are promising features of integrating PCMs into photonic devices.[18]

2 | PHASE TRANSITION AS OPTICAL MODULATION

Phase-change materials have introduced a new paradigm in optics: solid-to-solid phase transitions as a mechanism for optical modulation. Owing to their distinct optical properties, the switching of a PCM between the amorphous and the crystalline states leads to tunable optical response in a variety of optical devices. To understand this mechanism, it is paramount to understand the underpinning mechanisms for both crystallization and amorphization (i.e., melt-quenching). In the crystallization process, an external and localized thermal stimulus converts sub-critical nuclei in the amorphous matrix into super-critical nuclei, which will evolve into a larger grain of a thermodynamically favored state.[19] The glass transition temperature (T_g) determines the thermal stability (i.e., retention of properties) of PCMs in the amorphous state, and thus high T_g is desired. However, this behavior naturally contradicts the crystallization rate (R_{cry}). Note that T_g is the separation of high viscosity state and low viscosity state in glass solids while crystallization temperature (T_c) is the transition temperature from glass solids to crystalline. For amorphization, the external stimulus needs to exceed the melting temperature (T_m) followed by quenching faster than its critical cooling rate (R_{cool}). The supercooled liquid will rapidly be quenched and form a glassy solid phase. In practice, a relatively low T_m is desired to decrease the energy required to switch. The crystallization process is dictated by the rate at which atoms flip between different coordination states,[20] which is the process that ultimately limits the programming speed, given that melt-quenching, that is, R_{cool}, has to be faster to beat the crystallization process. A comparison of experimental timescales is shown in Figure 1A where we show the temporal evolution of the temperature during amorphization and crystallization.

Phase transformation in the most common O-PCMs consists mainly of two conjugate stages: nucleation and growth. PCMs are classified into two categories by their material properties, independent of switching methods: 1. Nucleation dominated: crystallization occurs through the formation of nuclei in "random" locations of amorphous matrix. As temperature increases, nuclei grow until they impinge on each other. Such materials, such as $Ge_2Sb_2Te_5$,[21] with nucleation faster than crystallization, can be switched in a few nanoseconds. 2. Growth dominated: only one "single" nucleus among a few nuclei precipitate in the amorphous matrix can potentially grow to complete crystallization. Such materials, including $Ag_3In_4Sb_{76}Te_{17}$[22] and Ti-doped Sb_2Se_3,[23] prefer to grow directionally from the crystalline-amorphous interface into the bulk with a growth rate larger than nucleation rate, as shown in Figure 1B. Despite many interfacial and dimensional factors associated with kinetics, the growth-dominated crystallization process usually takes longer due to significant activation energy. Recrystallization via either mechanism has a certain level of dependence on the stochastic spatial distribution of nuclei and their temporal evolution. Therefore, designing the composition of PCMs and engineering the external stimulus that induces phase transformation to tailor the device for various applications is inevitable yet challenging.

The contrast in optical properties between amorphous and crystalline states results from unconventional bond breaking and sharing of about one electron between adjacent atoms, coined as metavalent bonding.[24] The optical response from a PCM thin film or device, which can be observed as, for instance, transmission change and phase shift, all originate from the contrast in the real (n) and imaginary (k) parts of refractive indices of the PCM upon phase transformation. Figure 1B,C shows the index modulations, $\Delta n = n_{crys} - n_{am}$ and $\Delta k = k_{crys} - k_{am}$, that could be achieved in different spectrum ranges using the PCM Sb_2Se_3. Consider, for instance, embedding a patch of Sb_2Se_3 into a photonic waveguide, a pure amplitude modulation could be observed given that Sb_2Se_3 has $\Delta n = 0$ and $\Delta k \neq 0$ at $\lambda = \sim 300$ nm. Contrarily, pure resonance phase shift can be attained in the $\lambda > 1200$ nm regime as the Δk for Sb_2Se_3 goes to zero and $\Delta n > 0$, like demonstrated in elsewhere.[5] Both phase and amplitude modulations coexist in other bandwidths and together can be exploited in structural color.[9]

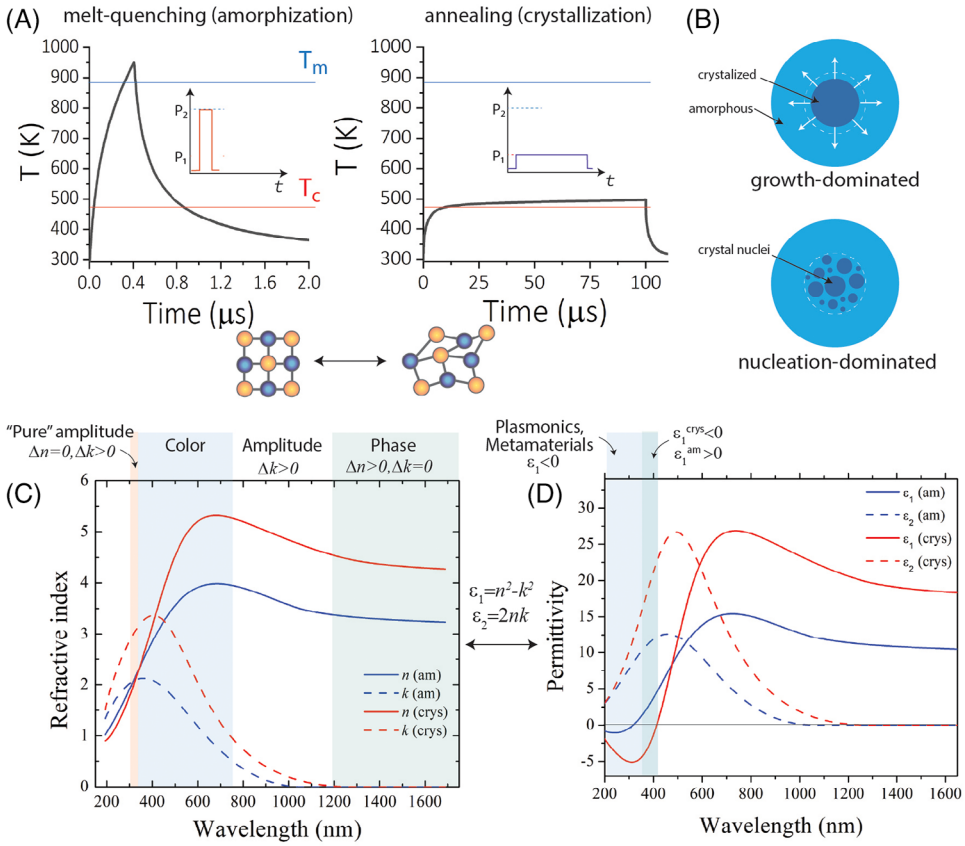

FIGURE 1 Reversible phase transition and optical properties modulation. (A) Illustration of the phase transition mechanisms. Crystalline phase change materials (PCMs) are melted at a temperature higher than T_m and quenched rapidly to a temperature below T_c in the amorphization process, which requires a short, powerful pulse. For crystallization, PCMs are annealed at a temperature slightly higher than T_c for a relatively longer period. (B) Diagram of recrystallization evolution for growth-dominated and nucleation-dominated mechanisms. (C) Shows refractive indices of Sb_2Se_3 in both states, highlighting different regions with properties leading to different applications. (D) The electrical permittivity of Sb_2Se_3 and potential applications of negative values and negative to positive trasitions.

The main advantage of PCMs is their nonvolatility. They can retain information with minimal power consumption when frequent switching is not required. Moreover, PCMs have greater long-term stability and can withstand drift when operating in the optical domain. This is because structural relaxation and long-range-order loss do not affect optical properties, while electrical readout has significant variability, particularly in amorphous state[25]—although this effect can be suppressed by using nanocomposites,[26] heterostructures,[27] bond reconfiguration,[28] and self-decomposition alternative.[29] Electric field-induced elemental segregation in PCMs is also avoided as current does not directly pass through the active material when operating fully in the optical domain.[30,31]

In addition to only the initial and final states, it is also important to understand that the optical constants evolve during nucleation, crystal growth, and melt-quenching. As a different ratio of glassy-crystalline domains results in multi-level optical constants, the effective dielectric function of intermediate PCM can be approximated from the following equation [32]:

$$\frac{\varepsilon_{eff}-1}{\varepsilon_{eff}+2} = f \times \frac{\varepsilon_c(\lambda)-1}{\varepsilon_c(\lambda)+2} + (1-f) \times \frac{\varepsilon_a(\lambda)-1}{\varepsilon_a(\lambda)+2}, \quad (1)$$

where f is defined as the crystallization fraction, $\varepsilon_c(\lambda)$ and $\varepsilon_a(\lambda)$ are the wavelength-dependent dielectric functions for crystalline and amorphous phases. Effective refractive indices can be transformed from the resultant effective dielectric function.

To avoid confusion, we are using the definition in optics in the following discussion by setting crystalline state as a baseline: write (amorphization), erase (crystallization), and read (passive measurements with low-power signal). To open our discussion, Table 1 semi-quantitatively summarizes the features of several different switching approaches in terms of reversibility, bits, speed, integration, resolution, uniformity, area, and energy consumption, regardless of the PCM employed.

TABLE 1 Overview of various switching methods used in photonic applications, that is, with optical readout. UH: Ultra-high; H: High, M: Medium, L: Low, UL: Ultra-low. N/A: Not applicable or not yet demonstrated or measured in an optical multilevel context. Speed refers to a full cycle of amorphous-crystalline-amorphous. Scalability is defined as the opportunity for a given method to be used in systems comprising many phase change material (PCM) elements. Uniformity is defined as the capability of a given method to produce uniform crystalline volumes such that the optical readout is significant.

Switching method	Approach	Reversibility[a] (cycles)	Levels[a] (bits)	Speed[a] (ns)	Resolution[a] (nm)	Scalability	Uniformity	*Energy
Optical	Free-space[32,33]	$>10^6$	4	$\sim10^1$	10^2	H	H	pJ-nJ
	On-chip[7,29]	10^6	6	$\sim10^2$	10^2	L	H	pJ-nJ
Electrical	Direct[34,35]	10^3	2	$\sim10^2$	10^1	H	L	nJ
	Indirect [6,36–39]	10^4 [b]	5	10^4-10^7	10^3	H	M	nJ-mJ
	Scanning probe[8,40–42]	N/A	3	N/A	10^1	L	M	mJ
	E-beam[43–45]	10^1	N/A	10^{10}	10^1	UL	L	200 keV[c]
Hotplate	–	N/A	N/A	N/A	N/A	N/A	UH	kJ

[a]Maximum number experimentally demonstrated.
[b]This number of cycles has been demonstrated only between two levels. Demonstrations with 64 levels (i.e., 5-bit) have not shown more than 10 cycles.[38,39]
[c]This refers to the accelerating energy of the electrons under a transmission electron microscope.[44]

3 | OPTICAL SWITCHING

O-PCMs can be switched using optical pulses at wavelengths above their bandgap, given that power from the pulses converts into the heat required to trigger the phase transformation. The power and width of the pulses are parameters that allow precise tunability by switching different O-PCM volumes, which in turn translates into a precise control of the optical response. This mechanism has long been explored using free-space lasers to switch between the amorphous and the crystalline states, which is, in fact, the mechanism used in rewritable compact disks.[33] More recently, a pump-probe mechanism with both pulses propagating inside a photonic waveguide was also proposed, as described in detail by Ríos et al.[46] An interesting feature of O-PCMs is their ability to "self-modulate" the energy they absorb, which leads to similar pulses triggering both amorphization and crystallization.[46] Other advantages of optical switching are achieving large area pattering for holograms [33,47] and high-speed switching with femtosecond laser.[48] When a beam is shone on PCMs, the energy carried by electromagnetic waves is dissipated as heat propagating through materials if the imaginary part of permittivity (ε'') is nonzero. The amount of heat being transferred to PCMs depends on the magnitude ε'', which quantifies the misalignment between dipoles and applied electric field. The heat then dissipates, creating a temperature gradient. This way, the heat transfer in the PCM is coupled to its optical properties[49]:

$$Q = \frac{1}{2}\omega\varepsilon''\vec{E}\cdot\vec{E}^* = \rho Cp\,\frac{dT}{dt} + \nabla\cdot(-\kappa\nabla T), \qquad (2)$$

where here Q refers to the heat source, ω is the optical frequency, $\vec{E}$ is the electrical field, is Cp the specific heat capacity at constant pressure, κ is the thermal conductivity of materials. Note that the intrinsic properties in the equations are all temperature dependent, that is, $\varepsilon \to (T)$, $\rho \to (T)$, $k \to (T)$ and $Cp \to (T)$. In particular, O-PCMs are well-known for displaying strong thermo-optical coefficients for temperatures below the crystallization temperature.[50]

3.1 | Free-space laser switching

Assuming a monochromatic Gaussian beam focusing onto the O-PCM, light is absorbed, and since such absorption depends on the incoming power, the heat profile also adopts a Gaussian shape. Phase switching is triggered within the area that reaches the transition temperature, that is, T_c or T_m. The wavelength of laser pulses chosen depends on the PCMs' bandgap. However, visible light can be used to switch most known PCMs, which display a large extinction coefficient in this spectral range.[51] Crystallization is usually realized by a sequence of medium-powered pulses while amorphization relies on a single high-power pulse, as sketched in Figure 2A, for free-space switching and free-space readout. Using these techniques, the glassy-crystalline domains can be varied in space by tuning the laser to pattern different spot sizes, for instance, amorphous domains within a fully crystallized film, as shown in Figure 2B. The size of the domains and whether growth occurs determines the total optical response in the form of higher or lower reflectivity[33] or change in color,[32] as shown in Figure 2C,D.

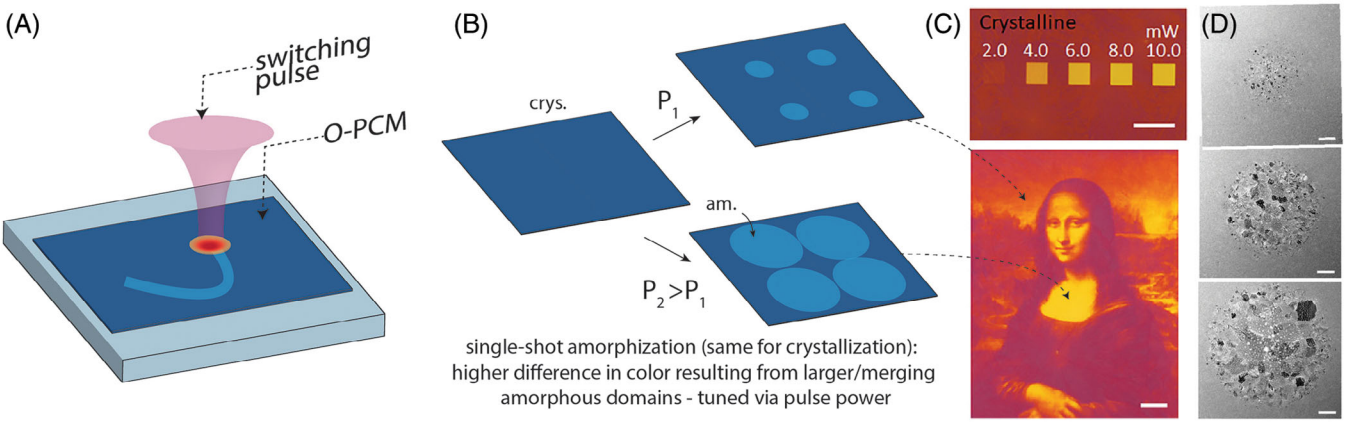

FIGURE 2 Free-space laser switching. (A) Sketch of the Gaussian hotspot due to laser heating on an optical phase change material (O-PCM) thin film. Arbitrary patterns can be transferred onto the O-PCM by controlling the pulse power and thus, the size of the amorphous/crystalline domain, as shown in (B). (C) Experimental demonstration of multi-level (gray-scale) color on Sb2S3 thin films (reproduced from 33), the scale bar equal is 20 μm. (D) Micrograph displaying a polycrystalline domain in amorphous material with increasing size as a function of laser power, from the top down: 2.8, 3.8, and 4.9 mW. The scale bar is 200 nm (reproduced from 32).

Recently, the field has shifted to increasing the density of information storage using free-space laser by either facilitating sub-diffraction limited features[52] or gray-scale under different levels of partial crystallization.[53] Wang et al. showed the recipe of using 532 nm and 5 ns pulse with different energy densities and number of pulses to partially crystallize (30 mJ/cm^2) and amorphized (56 mJ/cm^2) $Ge_2Sb_2Te_5$, realizing 4-bit in a single device.[53] Many applications were demonstrated using this approach, for example, bio-inspired computing,[54] optically reconfigurable metasurfaces[55] highly confined surface phonon polariton,[56] infrared antennas,[57] etc. Free-space laser in visible wavelength is also an alternative to switch low-loss PCMs, for example, Sb_2Se_3[58] and $Ge_2Sb_2Se_4Te_1$,[59] for telecommunications wavelength applications as on-chip alloptical operation is not viable, as explained in the next section. Nonetheless, this approach is constrained by the scalability, design flexibility and compactness of photonic integrated circuits (PICs).

3.2 | On-chip waveguide integrated

PCMs can applied in PICs, and their microstructure can be tuned using a pump-probe switching and readout protocol, as shown in Figure 3A. Instead of using direct incident light beams as in free-space switching, light is confined in low dimensional on-chip waveguiding structures and evanescently coupled to the PCM placed on the cladding. The attenuation of light propagating inside the PICs can be considered as the interaction between the electrical field and absorptive medium, given by $\alpha_{dB}(\lambda) = 4.34 \cdot \frac{4\pi}{\lambda}\kappa_{eff}(\lambda)$, where κ_{eff} is the effective extinction coefficient. The coupling to crystalline PCMs is usually stronger due to high extinction ratios, and thus, the absorbed power is higher than that of amorphous. As a consequence, and considering that similar wavelengths are desired for both switching and readout to reduce device complexity, only absorptive materials, such as $Ge_2Sb_2Te_5$ can be switched with this technique in the C-L telecommunication bands where most of the PIC work takes place.

In this technique, the PCM is initially prepared in a fully-crystalline state following an annealing process after deposition. This way, a reliable baseline for optical response is established, as opposed to relying on as-deposited amorphous, a unique and non-repeatable state.[50] In the switching process, ultrafast thermo-optical response takes place. The transmission initially decreases during the pulse excitation and then increases to set in its final state as the PCM cools down. The cooling time needs to be considered because readout must happen after the material microstructure forms and stabilizes. The size of the amorphous domain, which adopts a parabolic-like shape due to the asymmetry of the light-PCM interaction (see Figure 3A–D) can be controlled by experimentally tuning the pulse energy, that is, the power and length of the switching pulse. Likewise, a transient thermo-optical effect is observed in the recrystallization process. In this step, however, the switching is done either by steps or by engineering a double-stepped pulse[17] because the amorphous domain displays lower absorption than the surrounding crystalline PCM. Thus, heating takes place predominantly at their interface. Hence, nucleation takes place from the border of the amorphous domain and

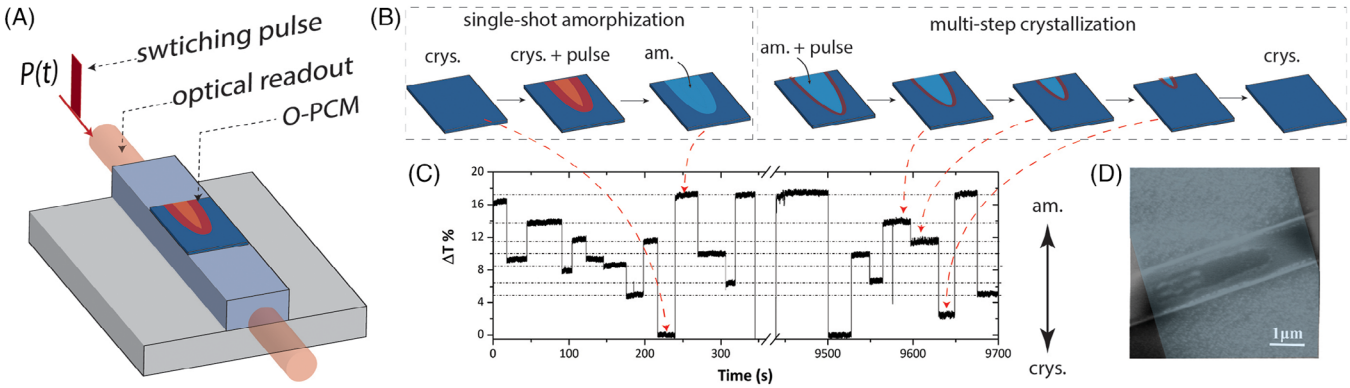

FIGURE 3 Laser switching inside a waveguide. (A) Sketch of the device with a parabolic-shaped hotspot resulting from the absorption of a switching pulse. The hotspot is asymmetric, starting from the side of incidence and reducing in size as the pulse is absorbed. (B) Amorphization and crystallization processes. In the amorphization, the melt-quenched area corresponds directly to the parabolic-like shape where T > Tm. During the crystallization, nucleation takes place at the edge between the amorphous and the crystalline domains, given the stronger optical absorption of the latter. (C) Experimental demonstration of reversible, multi-level, and reliable switching of Ge2Sb2Te5 on a silicon nitride waveguide. The amorphization (upwards) can be precisely done in steps since the hotspot size can be tuned via pulse power modulation. (D) Colored micrograph of the waveguide used in (C) with a parabolic-like amorphous domain embedded in crystalline Ge2Sb2Te5 (in blue).

advances into the crystalline region, one step at a time, as depicted in Figure 3B. This process, while energy and time-consuming, allows for precise control of the optical response as the process can be stopped at any intermediate step. Details about the experimental setup/process to pump laser pulses and measure transmission fully on-chip are elaborated by Ríos et al.[60]

4 | ELECTRICAL SWITCHING

Electrical switching adds another degree of freedom in reconfiguring PCMs for optical applications. Additionally, this switching mechanism bridges the gap between photonic devices and conventional electronics for seamless scalability and compatibility. This mechanism relies on resistive heating to control the state of the PCM. It can broadly be classified into two groups: 1. Direct Joule heating, where current is directly passing through the PCM itself, for example, cross-bar memories,[61] or 2. Indirect Joule heating, where the PCM is electrically isolated but in thermal contact with another material undergoing resistive heating, like a microheater.[62] Indirect joule heating has the benefit of heating large areas with high uniformity, which is most desired in photonic applications where large modulation in the glassy-crystalline domains is necessary to induce a significant optical modulation. On the other hand, direct Joule heating is more energy efficient; however, it results in crystalline filaments, which are too small compared to the wavelength and thus hinder any optical modulation. In a nutshell, the electrical power that converts to thermal power through Joule heating is obtained by combining Maxwell's equations and the heat diffusion equations. The temperature distribution in homogeneous materials can be expressed by[63]

$$\frac{dP}{dV} = \rho C_p \frac{dT}{dt} - \kappa \nabla^2 T = \frac{J^2}{\sigma(T)}, \tag{3}$$

where $\frac{dP}{dV}$ is the power per volume, ρ refers to the density of materials, C_p is the heat capacity, κ is the thermal conductivity of materials and σ is electrical conductivity. The temperature-dependent conductivity is important as the transition temperature of PCMs is high and varies from alloys to semiconductors. Joule heating in PCM also has a unique characteristic—threshold switching—current flowing in amorphous has nonlinear behavior as applied electric field increases. When the threshold voltage is reached, the conductivity drastically increases. Heat dissipation along the fast-current flow enables fast crystallization and reversible switching at relatively low voltages.[64]

4.1 | Direct Joule heating

In this method, power is transferred directly into PCM in a current-driven scheme; besides, the metal electrodes having thermal contact with PCM can be engineered as resistive heaters to control thermal gradients.[65] Nonetheless, the volume of materials that can be reversibly switched via filamentation is constrained owing to the short circuits forming between electrodes, leading to very limited optical contrast in photonic devices. The

electric field required for threshold switching also leads to close spacing between two electrodes, which further introduces optical loss. Despite the challenges and limitations of direct heating, there have been several applications. Zhang et al. demonstrate waveguide transmission with electrically-driven PCMs.[34] Also, combining PICs and plasmonic structures, strong light-matter interaction is enhanced in a highly confined region of PCMs. The optical mode size approaches similar dimensions to the filaments that are switched within a nanogap by direct electrical excitation, and thus, the interaction and optical modulation are enhanced. This opens new opportunities for mixed-mode design (optical/ electrical switch and optical/ electrical readout), which will be discussed in Section 5.

4.2 | Indirect Joule heating

Indirect joule heating improves the design flexibility by using thermally robust materials as thermal contact in an electro-thermal switching scheme. The major challenge using "microheaters" is endurance arising from mechanical failure of heaters and the void formation at the interface of heater and PCMs owing to thermal expansion during phase transition.[66] Note that a maximum cyclability of 103 has been demonstrated using indirect Joule heating while the direct Joule heating counterpart is several orders of magnitude higher.[67] From a materials selection perspective, conductive materials with high melting points are required to build the microheater; additionally, specific optical responses can be imposed on the microheater itself, for example, transparent versus reflective only. On the PCMs side, low transition temperatures are desired to minimize the power consumption and thermal fatigue of the entire device. Moreover, the film quality of PCMs plays an important role in minimizing defects and maximizing uniformity.

Metal heaters are commonly used because of their high conductivity, high melting temperature, and thermal properties. They are especially useful in reflective applications. Zhang et al. demonstrated using Pt microheaters with a Ti adhesion layer to switch $Ge_2Sb_2Se_4Te_1$ pixels over 103 cycles.[68] Castillo et al. also showed that microheaters are plausible in large-area switching by integrating them with a $50 \times 50\ \mu m^2$ thin-film transistor display.[69] Yet, metal heaters cannot be used in transmissive reconfigurable photonic devices. Transparent heaters, for example, ITO [70] and Ga:InO,[71] are alternative candidates as they are also conductive, thermally stable, and most importantly, less absorptive in visible to near-infrared windows. Youngblood et al. showed switching of GeTe[72] using FTO heaters, which is limited in its programming speed, given that conductive oxides are usually 2–3 orders less thermally conductive than metals. In such heaters, the heat dissipation hinders both fast crystallization and melt-quench, and only slow PCMs, that is, PCMs with crystallization kinetics in the microsecond time scale, such as GeTe or $Ge_2Sb_2Se_4Te$ can be selected.

Taking advantage of well-developed CMOS processes in foundries, silicon is another robust alternative. On one hand, silicon has a high melting temperature and relatively large thermal conductivity. Doping silicon to increase its electrical conductivity creates a route to precisely engineer temperature gradients directly on silicon photonic waveguides, that is, the waveguide itself is part of the microheater, as demonstrated by Ríos et al.[5] High dopant concentrations decrease the resistivity and heating will occur in the lower resistivity regions defined by geometries, for instance narrow bridges with n doping sandwiched by two relatively low-resistive contacts n^{++}.[5] With single-element doping, it can also be extended to $p^{++}/p/p^{++}$ design.[73] It is worth noting that higher doping increases heating efficiency at the cost of larger optical loss due to free-electron absorption.[74] Another way to minimize insertion loss is by using p-i-n diode heaters since the undoped silicon waveguide can be used as the intrinsic region. Zheng et al. demonstrated this design featuring similar insertion loss compared to low n-doped $n^{++}/n/n^{++}$ microheaters, with lower operational voltages but similar power consumption since p-i-n becomes highly conductive under forward bias.[75]

When embedding these microheaters into photonic waveguides (see Figure 4A), the amorphization has been done in a single or double step since most of the PCM cell is heated over the T_m simultaneously, as shown in Figure 4B. Controlling the size of the amorphous domain inside a crystalline film in a similar manner as optical switching is challenging but could be realized by engineering the heater geometry to control its thermal profile. Optical tunability using this method was demonstrated by Ríos et al.[5] using multiple bridged heaters, that is, using five sections as opposed to a single larger (typically a bow-tie geometry) conductive pad. Similarly, crystallization takes place over the entire PCM volume by randomly distributed nucleation, forming nuclei that grow and merge to form a predominantly crystalline domain, as depicted in Figure 4B. While the crystallization process can be stopped at intermediate glassy-crystalline distributions, the random nature of the crystalline nuclei makes electrical switching less reliable in attaining precise and reproducible multilevel states, as shown in the experimental data in Figure 4C (compared to similar modulation in Figure 3).

The microheaters can also be used in free-space optical applications, as shown in Figure 5A. In this case, one of

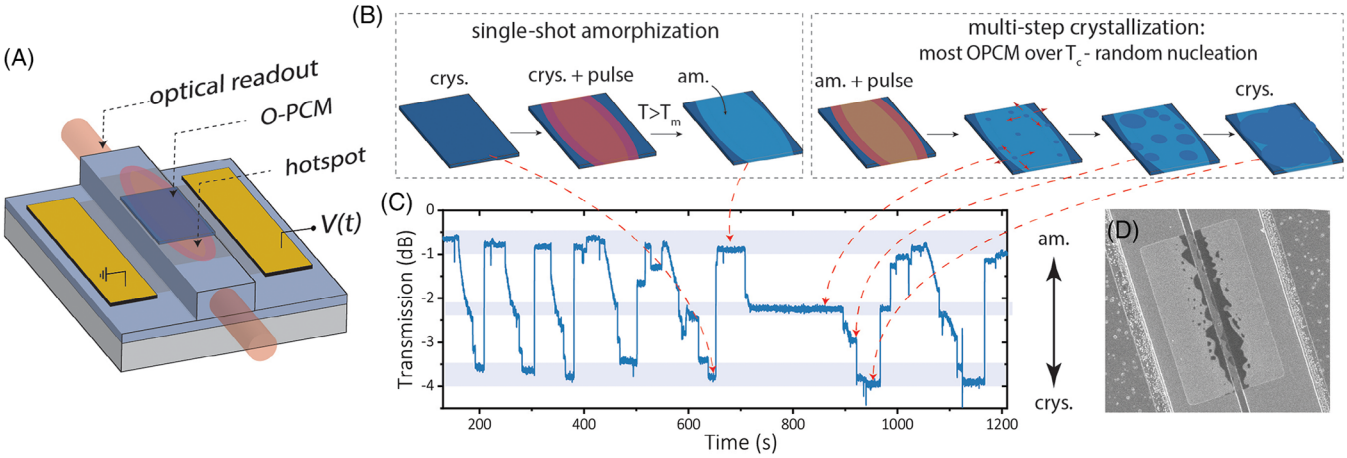

FIGURE 4 Waveguide integrated microheater. (A) Schematic of a doped-silicon microheater, in which the same silicon is both the waveguide and the heater element. (B) Amorphization and crystallization processes defining the glassy-crystalline domain distributions. Note that the geometry of the doped area determines the hotspot profile and dimensions. (C) Experimental transmission by electrically switching Ge2Sb2Se4Te on silicon-on-insulator waveguides, measured at 1550 nm. (D) Scanning electron microscopy (SEM) micrograph of a device cycled several times and finally ablated. The ablated area coincided with the waveguide, where the hotspot was predicted to extend over the entire length of the PCM cell.

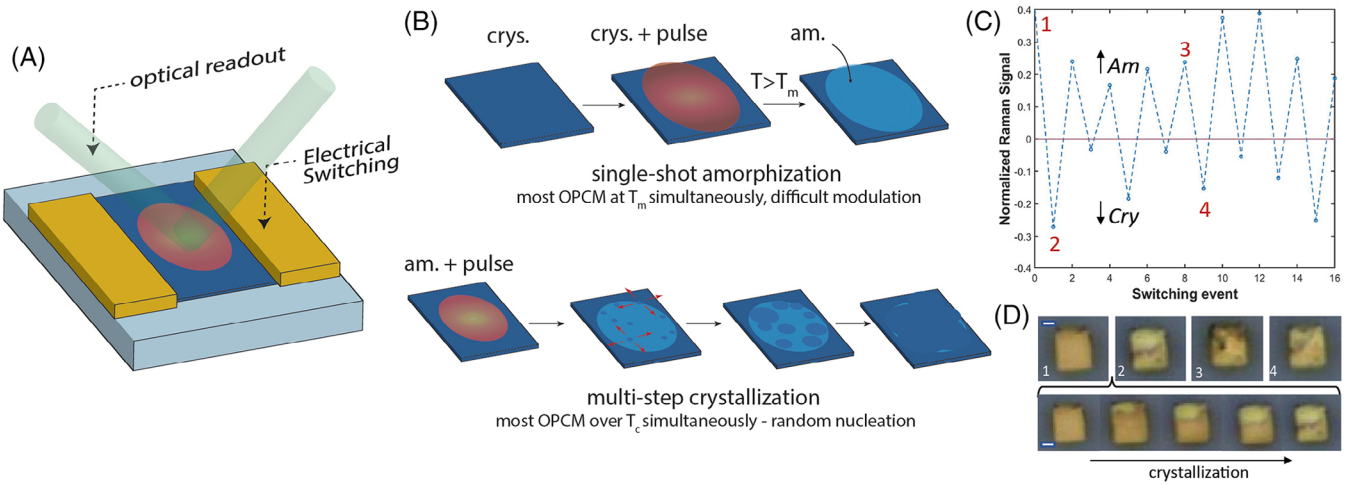

FIGURE 5 Large area microheater for free-space applications. (A) Schematic of microheater with PCM and free-space optical readout. (B) Amorphization and crystallization processes defining the glassy-crystalline domain distributions—similar to those in Figure 4C) Raman signal for crystalline (120 cm^{-1}) and amorphous (160 cm^{-1}) Ge2Sb2Se4Te upon reversible switching. (D) Optical microscope images of the Ge2Sb2Se4Te cell after different switching events. Points 1–4 refer to those labeled in (C). The lack of uniformity on the surface displays the random nature of both amorphization and crystallization, which, as observed in (c), prevents attaining reliable intermediate glassy-crystalline distributions.

the most challenging aspects is having large areas (> 25 μm^2) with a power consumption that increases quadratically with the side length of the heater. For such a task, metal heaters have demonstrated the best performance.[12] In addition, 2D materials have also been proposed, given their superior optical, electrical and thermal properties, an excellent alternative, particularly in applications requiring transparent heaters. For example, Rios et al. showed a patterned single-layer graphene applied on a SiO_2 substrate for $Ge_2Sb_2Se_4Te_1$ using 7.5 V/13μs pulses for amorphization and 6 V/20 ms for crystallization.[76] However, such a device displays a strong scattering of surface polar phonons, which affects heat dissipation and limits the heating/cooling speeds. Consequently, like conductive oxides, the PCMs that can be switched are those with slow crystallization kinetics in the microsecond time scales. In terms of glassy-crystalline domain distributions, the amorphization and crystallization follow a similar pattern as

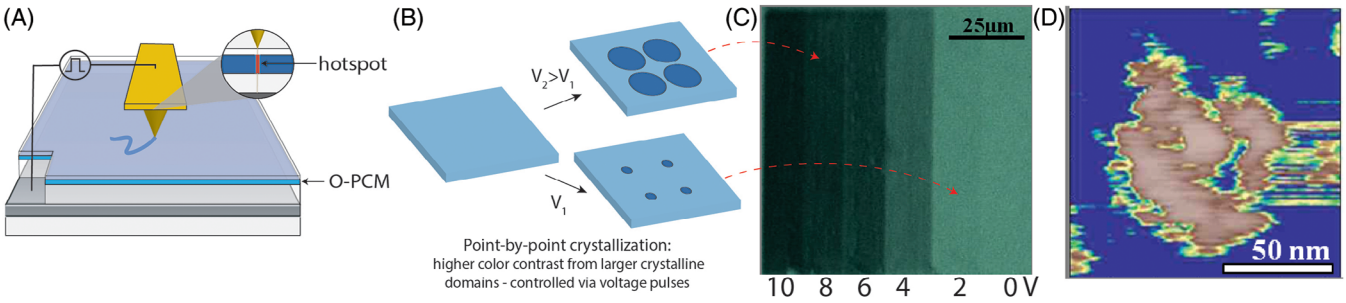

FIGURE 6 Crystallization via conductive atomic force microscopy. (A) Sketch of the setup to locally crystallize thin films of phase change material (PCM) using conductive atomic force microscopy (c-AFM). (B) Crystalline domains in amorphous films grow as a function of the pulse voltage applied using c-AFM. The glassy-crystalline domain ratio will depend on the size of the crystalline nuclei and whether they merge or not to form a stronger color. (C) Experimental demonstration of gray-scale color writing using pointillism-like visual effects at the macroscale. (D) c-AFM imaging of a single nuclei on AIST by applying a 10 V pulse.

the integrated microheater in Figure 5. The main difference lies in the difficulty of engineering the heat profile by modifying the geometry significantly. Because of this, amorphization is again relegated to a single-step process, while multilevel relies on random nucleation processes throughout the entire surface, thus hindering the precise and repeatable multilevel response. Another issue with these microheaters is that the amorphization process is a violent event in which, after several cycles, all the nuclei can disappear, thus preventing further recrystallization and leading to device failure. An alternative to this issue is having a PCM section outside the microheater that is never heated above T_m and is connected to the active area in a way that nucleation can take place from its always crystalline state.[77]

4.3 | Scanning probe lithography and electron-beam switching

Besides conventional electrical switching methods, scanning probe lithography provides a path to locally modify the properties of PCM thin films, as depicted in Figure 6A. This technique enables ultra-high-resolution pattering down to tens of nanometers (see Figure 6D). Analogous to direct joule heating, conductive atomic force microscopy (c-AFM) has been used to pattern PCM thin films by applying current between the probe and a grounded sample to create crystalline filaments. By using different voltage biases, a pointillism-like gray-scale modulation of colors, as demonstrated by Ríos et al. [8] and shown in Figure 6B,C. Despite the ultra-high resolution, this technique is limited to conductive substrates, which is not necessarily the case for dielectric metasurfaces and most PICs. Also, reversible switching is yet to be demonstrated. Thermal scanning probe, a similar technique using the concept of indirect joule heating and employing a resistive-heating probe, has been used to locally heat and crystallize 30 nm thick GeTe films[40] and 30 nm $Ge_2Sb_2Se_4Te$.[41] A Multiphysics simulation showed the prediction of local crystallization down to tens of nanometers.[42] In spite of the fact that this substrate-blind approach resolves the substrate limitation of c-AFM, the switching uniformity is a concern when the sample being switched is thick since only the topmost part will undergo crystallization.

Another even higher-resolution technology to pattern PCMs is e-beam, which enables localized crystallization and amorphization down to sub-10 nm resolutions. Studies have shown electron irradiation-induced crystallization in GaSb and Ge-, In-doped SbTe PCMs using a 120 kV beam[43] and $Si_2Sb_2Te_5$ thin films using a 100 kV system with a current density of 100 pA/cm2 and exposures of 10 min.[45] Moreover, Jian et al. demonstrated reversible switching in $Ge_2Sb_2Te_5$ without melt-quench.[44] Despite the ultra-high resolution, e-beam techniques suffer from massive energy consumption and long exposure time, which further limits large-scale patterning.

4.4 | Mixed-mode

Most PCMs display strong electrical/optical contrast during phase transition. For example, $Ge_2Sb_2Te_5$ has a change in electrical conductance of more than four orders of magnitude, while in the extinction coefficient can be 5 times larger in the near-infrared.[78] Although the context focuses on optical readout, optical and electrical information can be decoded from PCMs. For data encoding, optical and electrical switching can be applied simultaneously, assuming the PCM is reconfigurable from both domains. New "mixed-mode" devices are proposed and believed to facilitate emerging applications requiring conversions between these two domains. It is obvious that the degree of freedom is highly enhanced with this hybrid design. However, it is

also worth noting that it might potentially inherit both pros and cons from both domains.

PCM nanowires show improved thermal stability, lower melting temperature, and better crystallinity than their thin-film analogs. Therefore, they are good candidates for photonic waveguide integration with electrical and optical control. Lu et al. suspended GeTe nanowires between two contacts on Si_3N_4 waveguides and detected both the optical transmission and electrical conductance.[79] However, the cyclability of such a device is limited and electrical control is not yet demonstrated. The major challenge of using direct joule heating is the limitation of switching volume and, thus, having insignificant refractive index contrast. To solve this, plasmonic-enhanced devices have been proposed, using a plasmonic waveguide to confine the mode on a smaller area where a filamentation process occurs in a nanogap between two metal contacts.[79,80] It is a comprehensive mixed-mode realization, although further work needs to be done to engineer reliable switching and readout and further reduce the optical losses.

5 | PROGRAMMING STRATEGY

Independent of the reconfiguration approach, back-and-forth switching must be precise and repeatable between crystalline, amorphous, and intermediate states. Establishing a reliable operative "recipe" regardless of the switching mechanism is key, as proposed by Ríos et al.[60] Electrical and optical switching methods allow the progressive crystallization that displays both threshold and accumulation, which are core nonlinear responses to the realization of synapses[81] and neurons.[3] Moreover, they display a linear property modulation between threshold and accumulation that can be used for in-memory computing.[54] Multi-level operation in these and other applications is crucial and can be achieved by controlling the number and energy of the pulses depending on the initial and the target states. Ideally, any level should be attainable with a single-shot crystallization or amorphization stimulus, as done optically with remarkable precision. A two-step operation, that is, full amorphization followed by partial crystallization, is, however, still necessary for those mechanisms in which single-short amorphization cannot achieve intermediate levels since the entire PCM cell is amorphized at once. A way to circumvent the latter situation is using a double-step single-pulse programming scheme, as shown in the optical domain by Li et al.[17] This approach allows programming any targeted level independent of the prior state by always melt-quenching and controllably annealing to achieve the precise glassy-crystalline ratios. While this is still to be demonstrated in electrical switching, it can be an avenue to overcome the single-shot amorphization limitation imposed by having the entire PCM reaching T_m simultaneously, although energy-demanding and fatigue-inducing melt-quenching is required in every event.

Another strategy to increase the cyclability of devices is through material conditioning. This is, devices must be trained by cycling several times, under the same condition, until stable minimum and/or maximum values are found and repeatable behavior attained. Besides optimizing programming procedures, it is important to restrain any possible material inhomogeneity and segregation stemming from multiple switching events. To do so, a proven mechanism has been encapsulating PCMs with inert and stable materials by suppressing undesired interdiffusion, oxidation, and dewetting.[82] Ideally, designing PCMs that are robust against cyclic stress and thermal expansion/compression will be the desired solution.

6 | OPEN CHALLENGES

PCMs for photonics have a bright future, which is already reflected in the increasing number of publications and active research on the topic. To reiterate, precise switching plays a major role in the correct optical response for any application. While we have highlighted various approaches and devices to do so, there is still plenty of work to do before PCMs can reach maturity and be used in technology-ready optical systems. Here, we identify some of the pending challenges and discuss potential strategies to overcome them.

6.1 | Multi-level control

As mentioned extensively in Section 5, many applications are pursuing higher and higher information density in a single device nowadays. The accumulative and analog nature of PCM is attractive, but it relies on precise control of intermediate states via deterministic glassy-crystalline domain distributions. The states have to be reliable and cyclable. Ideally, bi-directional multi-level is desired; however, crystallization is intrinsically stochastic, arising from the randomness of nuclei distribution and growth, especially during electro-thermal switching. An alternative is to focus on multi-level modulation via amorphization instead. This is, in fact, the key ingredient in the successful optical switching in photonic waveguides (see Figure 3). It is relatively easy to engineer the hotspots by controlling device parameters (e.g. the shape of the heater, the pulse energy, etc.) and guarantee deterministic areas that will undergo melt-quenching as long as they are heated over T_m and provided proper material conditioning.[5]More

in-depth numerical models will also help understanding the dynamics behind the precise control of glassy and crystalline domains.[32]

6.2 | Path to scalability/cyclability

Although the choice of switching method highly depends on the application and the PCMs of choice, it is worth noting that microheaters are the most promising route to a seamless, scalable platform (i.e., a platform in which hundreds or thousands of PCMs can be switched in the same system). Microheaters are compatible with silicon-based platforms and inherit the maturity of CMOS technology for on-chip integration. Nevertheless, and despite the potential in terms of scalability, the state-of-the-art devices show poor endurance and cyclability (~103 cycles) in comparison to all-optical approaches using the same materials (~107 cycles). The underlying failure mechanisms are highly understudied, and it is imperative to know their mechanisms to design failure-resistant devices and materials. Lastly, higher operation speed, precision in attaining a given intermediate level, and switching uniformity in large-area PCMs require significant research efforts to bring such materials to real-world applications territory.

6.3 | New materials and better characterization data

There are many trade-offs when selecting PCMs and switching mechanisms, as shown in Table 1. The selection of the right PCM depends ultimately on the application and, obviously, on the available alloys. The field should move toward populating an optical PCM library with tailored properties for specific applications but, more importantly, characterizing thoroughly their optical, electronic, and thermal properties—the chalcogenide materials currently available are limited in number, and so is the relevant characterization data given the strong research focus on device and applications, many of which use empirically developed switching mechanisms. Understanding the crystallization dynamics and, crucially, the thermal properties of ultra-thing PCMs is necessary to engineering any type of robust and reliable device.

In terms of application, it is important to develop new alloys with sought-after properties at specific spectral windows (see Figure 1); namely, large refractive index, large/vanishing extinction coefficient, positive/negative permittivity, index contrast, etc. Ranging from single elements to quaternary alloys and beyond, the combinatorial space is huge and still highly unexplored. Important aspects of developing novel materials are to solve open challenges in the current ones while displaying strong optical modulation:

1. Restraining element segregation and oxidation upon switching towards highly cyclable devices. These are usually prevented using capping layers,[82] but the challenge of finding solutions from a materials design point of view remains open.
2. Find PCMs with small or no volumetric changes upon switching. Alternatively, find mechanisms to prevent volumetric expansion, like demonstrated recently via capping layer thickness control.[83] This is crucial to avoid mechanical variations that impact the lifespan and cyclability.
3. Energy consumption during switching by developing, for instance, PCMs with lower crystallization and amorphization temperatures; a challenge that has been approached via doping of conventional PCMs.[82]
4. PCMs with slow crystallization kinetics for reversible switching of thick (> 500 nm) structures, for example, metasurface for tunable free-space optics, like those achieved recently using $Ge_2Sb_2Se_4Te$.[12,68]
5. PCMs with fast crystallization kinetics for high-speed switching applications—can a PCM outperform $Ge_2Sb_2Te_5$ while displaying repeatable and strong optical modulation? Fast switching is pivotal for optical neural networks with low latency.[84]
6. Developing PCMs with large bandgaps towards visible wavelength modulation; like proposed recently moving away from tellurides to selenides and sulfides.[16] Such alloys could open new horizons to PCMs, for instance, in quantum photonics.
7. Broadband transparent PCMs with large index contrasts, ideally spanning into the visible wavelengths. A precedent is the telluride-selenide-based compound $Ge_2Sb_2Se_4Te$ for mid- and long-wave infrared.[68]
8. PCMs with high thermal stability and small/negligible thermo-optical effect for temperatures below the crystallization temperature. Such properties are important to achieve devices that can be operated in a large temperature range without distortion in the optical response.

ACKNOWLEDGMENTS

Carlos A. Ríos Ocampo acknowledges support from the U.S. National Science Foundation under Grants ECCS-2210168 and DMR-2329087, and the Minta Martin Foundation through the University of Maryland. Ichiro Takeuchi is supported by ONR MURI N00014-17-1-2661.

ORCID

Chih-Yu Lee https://orcid.org/0000-0001-7437-7343

Carlos A. Ríos Ocampo https://orcid.org/0000-0001-6859-5491

REFERENCES

1. Ovshinsky SR. Reversible Electrical Switching Phenomena in Disordered Structures. Phys Rev Lett. 1968;1(20):1450–53.
2. Raoux S, Xiong F, Wuttig M, Pop E. Phase change materials and phase change memory. MRS Bull. 2014;39(8):703–10.
3. Feldmann J, Youngblood N, Wright CD, Bhaskaran H, Pernice WHP. All-optical spiking neurosynaptic networks with self-learning capabilities. Nature 2019;569(7755):208–14.
4. Chen R, Fang Z, Miller F, Rarick H, Fröch JE, Majumdar A. Opportunities and challenges for large-scale phase-change material integrated electro-photonics. ACS Photonics. 2022;9(10):3181–95.
5. Ríos C, Du Q, Zhang Y, Popescu C-C, Shalaginov MY, Miller P, et al. Ultra-compact nonvolatile phase shifter based on electrically reprogrammable transparent phase change materials. PhotoniX. 2022;3(1):26.
6. Fang Z, Chen R, Zheng, J, Khan, AI, Neilson, KM, Geiger, SJ, et al. Ultra-low-energy programmable non-volatile silicon photonics based on phase-change materials with graphene heaters. Nat Nanotechnol. 2022;17(8):842–48.
7. Feldmann J, Stegmaier M, Gruhler N, Ríos C, Bhaskaran H, Wright CD, et al. Calculating with light using a chip-scale all-optical abacus. Nat Commun. 2017;8(1):1256.
8. Ríos C, Hosseini P, Taylor RA, Bhaskaran H. Color depth modulation and resolution in phase-change material nanodisplays. Adv Mater. 2016;28(23):4720–26.
9. Huang Yi-S, Lee C-Yu, Rath M, Ferrari V, Yu H, Woehl TJ, et al. Tunable structural transmissive color in fano-resonant optical coatings employing phase-change materials. Mater Today Adv. 2023;18:100364.
10. Hosseini P, Wright CD, Bhaskaran H. An optoelectronic framework enabled by low-dimensional phase-change films. Nature. 2014;511(7508):206–11.
11. Shalaginov MY, An S, Zhang Y, Yang F, Su P, Liberman V, et al. Reconfigurable all-dielectric metalens with diffraction-limited performance. Nat Commun. 2021;12(1):1225.
12. Zhang Y, Fowler C, Liang J, Azhar B, Shalaginov MY, Deckoff-Jones S, et al. Electrically reconfigurable non-volatile metasurface using low-loss optical phase-change material. Nat Nanotechnol. 2021;16(6):661–66.
13. Chaudhary K, Tamagnone M, Yin X, Spägele CM, Oscurato SL, Li J, et al. Polariton nanophotonics using phase-change materials. Nat Commun. 2019;10(1):4487.
14. Sreekanth KV, Ouyang Q, Sreejith S, Zeng S, Lishu Wu, Ilker E, et al. Phase-change-material-based low-loss visible-frequency hyperbolic metamaterials for ultrasensitive label-free biosensing. Adv Opt Mater. 2019;7(12):1900081.
15. Gholipour B, Karvounis A, Yin J, Soci C, Macdonald KF, Zheludev NI. Phase-change-driven dielectric-plasmonic transitions in chalcogenide metasurfaces. NPG Asia Mater. 2018;10(6):533–39.
16. Delaney M, Zeimpekis I, Lawson D, Hewak DW, Muskens OL. A new family of ultralow loss reversible phase-change materials for photonic integrated circuits: Sb2S3 and Sb2Se3. Adv Funct Mater. 2020;30(36):2002447.
17. Li X, Youngblood N, Ríos C, Cheng Z, Wright CD, Pernice WHp, et al. Fast and reliable storage using a 5 bit, nonvolatile photonic memory cell. Optica 2019;6(1):1–6.
18. Wuttig M, Bhaskaran H, Taubner T. Phase-change materials for non-volatile photonic applications. Nat Photonics. 2017;11(8):465–76.
19. Amini N, Pries J, Cheng Y, Persch C, Wuttig M, Stolpe M, et al. Thermodynamics and kinetics of glassy and liquid phase-change materials. Mater Sci Semicond Process. 2021;135:106094.
20. Sarwat SG. Materials science and engineering of phase change random access memory. Mater Sci Technol. 2017;33(16):1890–906.
21. Privitera S, Bongiorno C, Rimini E, Zonca R. Crystal nucleation and growth processes in Ge2Sb2Te5. Appl Phys Lett. 2004;84(22):4448–50.
22. Gille T, Goux L, Lisoni J, De Meyer K, Wouters DJ. Impact of material crystallization characteristics on the switching behavior of the phase change memory cell. MRS Online Proc Libr. 2006;918(1):6020702.
23. Wu T, Wang G, Lotnyk A, Zhu J, Jiao Y, Shen X. Development of Sb2Se3 alloys by Ti-doping with ultralow resistance drift and improved microstructure for nonvolatile memory applications. Appl Phys Lett. 2023;123(7):073102.
24. Zheng T, Hu X, He F, Wu Q, Han B, Chen Da, et al. Tailoring nanoprecipitates for ultra-strong high-entropy alloys via machine learning and prestrain aging. J Mater Sci Technol. 2021;69:156–67.
25. Zhang W, Ma E. Unveiling the structural origin to control resistance drift in phase-change memory materials. Mater Today. 2020;41:156–76.
26. Khan AI, Yu H, Zhang H, Goggin JR, Kwon H, Wu X, et al. Energy efficient neuro-inspired phase–change memory based on Ge4Sb6Te7 as a novel epitaxial nanocomposite. Adv Mater. 2023;35(30):2300107.
27. Khan AI, Wu X, Perez C, Won B, Kim K, Ramesh P, et al. Unveiling the Effect of Superlattice Interfaces and Intermixing on Phase Change Memory Performance. Nano Lett. 2022;22(15):6285–91.
28. Jiao Y, Wang G, Lotnyk A, Wu T, Zhu J, He A. Designing Sb phase change materials by alloying with Ga2S3 towards high thermal stability and low resistance drift by bond reconfigurations. J Alloys Compd. 2023;953:169970.
29. Zhu J, Wang G, Jiao Y, Wu T, Lotnyk A. Monatomic Sb thin films alloyed with Sb2S3 enables superior thermal stability and resistance drift by spontaneous self-decomposition. Ceram Int. 2023;49(12):19960–65. https://doi.org/10.1016/j.ceramint.2023.03.117
30. Xu Q, Lian E, Yeoh P, Skowronski M. Segregation-induced Ge precipitation in Ge2Sb2Te5 and N-doped Ge2Sb2Te5 line cells. AIP Adv. 2022;12(6):065018.
31. Joo Y-C, Yang T-Y, Cho Ju-Y, Park Y-J. Electromigration in molten-phase $Ge_2Sb_2Te_5$ and effects of doping on atomic migration rate. J Korean Ceram Soc. 2012;49(1):43–47.
32. Wang Y, Ning J, Lu Li, Bosman M, Simpson RE. A scheme for simulating multi-level phase change photonics materials. Npj Comput Mater. 2021;7(1):1–10.
33. Liu H, Dong W, Wang H, Lu Li, Ruan Q, Tan YS, et al. Rewritable color nanoprints in antimony trisulfide films. Sci Adv. 2020;6(51):eabb7171.

34. Zhang H, Zhou L, Xu J, Wang N, Hu H, Lu L, et al. Nonvolatile waveguide transmission tuning with electrically-driven ultra-small GST phase-change material. Sci Bull. 2019;64(11):782–89.
35. Rodriguez-Hernandez G, Hosseini P, Ríos C, Wright CD, Bhaskaran H. Mixed-mode electro-optical operation of Ge2Sb2Te5 nanoscale crossbar devices. Adv Electron Mater. 2017;3(8):1700079.
36. Popescu C-C, Dao KP, Ranno L, Mills B, Martin L, Zhang Y, et al. An open-source multi-functional testing platform for optical phase change materials. 2023.
37. Zhou W, Dong B, Farmakidis N, Li X, Youngblood N, Huang, K, et al. In-memory photonic dot-product engine with electrically programmable weight banks. Nat Commun. 2023;14(1):2887.
38. Wei M, Li J, Chen Z, Tang Bo, Jia Z, Zhang P, et al. Electrically programmable phase-change photonic memory for optical neural networks with nanoseconds in situ training capability. Adv Photonics. 2023;5(4):046004.
39. Chen R, Fang Z, Perez C, Miller F, Kumari K, Saxena A, et al. Non-volatile electrically programmable integrated photonics with a 5-bit operation. Nat Commun. 2023;14(1):3465.
40. Podpirka A, Lee W-K, Ziegler JI, Brintlinger TH, Felts JR, Simpkins BS, et al. Nanopatterning of GeTe phase change films via heated-probe lithography. Nanoscale 2017;9(25):8815–24.
41. Schwarz CM, Kuebler SM, Rivero-Baleine C, Triplett B, Kang M, Altemose Q, et al. Structurally and morphologically engineered chalcogenide materials for optical and photonic devices. J Opt Microsyst. 2021;1(1):013502.
42. Michel A-KU, Meyer S, Essing N, Lassaline N, Lightner, CR, Bisig S, et al. The potential of combining thermal scanning probes and phase-change materials for tunable metasurfaces. Adv Opt Mater. 2021;9(2):2001243.
43. Kaiser M, Van Pieterson L, Verheijen MA. In situ transmission electron microscopy analysis of electron beam induced crystallization of amorphous marks in phase-change materials. J Appl Phys. 2004;96(6):3193–98.
44. Jiang T-T, Wang J-J, Lu Lu, Ma C-S, Zhang D-Li, Rao F, et al. Progressive amorphization of GeSbTe phase-change material under electron beam irradiation. APL Mater. 2019;7(8): 081121.
45. Zhang T, Song Z, Sun M, Liu Bo, Feng S, Chen B. Investigation of electron beam induced phase change in Si2Sb2Te5 material. Appl Phys A. 2008;90(3):451–55.
46. Rios C, Stegmaier M, Cheng Z, Youngblood N, Wright CD, Pernice WHP, et al. Controlled switching of phase-change materials by evanescent-field coupling in integrated photonics [Invited]. Opt Mater Express. 2018;8(9):2455–70.
47. Zhou H, Wang Y, Li X, Wang Q, Wei Q, Geng G, et al. Switchable active phase modulation and holography encryption based on hybrid metasurfaces. Nanophotonics 2020;9(4):905–12.
48. Hase M, Fons P, Mitrofanov K, Kolobov AV, Tominaga J. Femtosecond structural transformation of phase-change materials far from equilibrium monitored by coherent phonons. Nat Commun. 2015;6(1):8367.
49. Haus HA, Melcher JR. Electromagnetic fields and energy. Upper Saddle River, NJ: Prentice Hall; 1989
50. Stegmaier M, Ríos C, Bhaskaran H, Pernice WHP. Thermo-optical effect in phase-change nanophotonics. ACS Photonics. 2016;3(5):828–35.
51. Arjunan MS, Durai S, Mondal A, Adarsh K, Manivannan A. Realization of 4-bit multilevel optical switching in Ge2Sb2Te5 and Ag5In5Sb60Te30 phase-change materials enabled in the visible region. ACS Appl Electron Mater. 2020;2(12):3977–86.
52. Hamann HF, O'boyle M, Martin YC, Rooks M, Wickramasinghe HK. Ultra-high-density phase-change storage and memory. Nat Mater. 2006;5(5):383–87.
53. Wang R, Wei J, Fan Y. Chalcogenide phase-change thin films used as grayscale photolithography materials. Opt Express. 2014;22(5):4973–84.
54. Ríos C, Youngblood N, Cheng Z, Le Gallo M, Pernice WHP, Wright CD, et al. In-memory computing on a photonic platform. Sci Adv. 2019;5(2):eaau5759.
55. Wu C, Yu H, Lee S, Peng R, Takeuchi I, Li Mo. Programmable phase-change metasurfaces on waveguides for multimode photonic convolutional neural network. Nat Commun. 2021;12(1):96.
56. Sumikura H, Wang T, Li P, Michel A-KU, Heßler A, Jung L, et al. Highly confined and switchable mid-infrared surface phonon polariton resonances of planar circular cavities with a phase change material. Nano Lett. 2019;19(4):2549–54.
57. Michel A-KU, Zalden P, Chigrin DN, Wuttig M, Lindenberg AM, Taubner T. Reversible optical switching of infrared antenna resonances with ultrathin phase-change layers using femtosecond laser pulses. ACS Photonics. 2014;1(9):833–39.
58. Delaney M, Zeimpekis I, Du H, Yan X, Banakar M, Thomson DJ, et al. Nonvolatile programmable silicon photonics using an ultralow-loss Sb2Se3 phase change material. Sci Adv. 2021, 7(25):eabg3500.
59. Vitale SA, Miller P, Robinson P, Roberts C, Liberman V, Du Q, et al. Phase transformation and switching behavior of magnetron plasma sputtered Ge2Sb2Se4Tephase transformation and switching behavior of magnetron plasma sputtered Ge2Sb2Se4Te. Adv Photonics Res. 2022;3(10):2200202.
60. Ríos C, Stegmaier M, Hosseini P, Wang Di, Scherer T, Wright CD, et al. Integrated all-photonic non-volatile multi-level memory. Nat Photonics. 2015;9(11):725–32.
61. Kau D, Tang S, Karpov IV, Dodge R, Klehn B, Kalb J, et al. A stackable cross point phase change memory. IEDM. 2009:1–4.
62. Abdollahramezani S, Hemmatyar O, Taghinejad M, Taghinejad H, Krasnok A, et al. Electrically driven reprogrammable phase-change metasurface reaching 80% efficiency. Nat Commun. 2022;13(1):1696.
63. Le Gallo M, Sebastian A. An overview of phase-change memory device physics. J Phys Appl Phys. 2020;53(21):213002.
64. Stern K, Wainstein N, Keller Y, Neumann CM, Pop E, Kvatinsky S, et al. Uncovering phase change memory energy limits by sub-nanosecond probing of power dissipation dynamics. Adv Electron Mater. 2021;7(8):2100217.
65. Russo U, Ielmini D, Redaelli A, Lacaita AL. Modeling of programming and read performance in phase-change memories—part I: cell optimization and scaling. IEEE Trans Electron Devices. 2008;55(2):506–14.
66. Popescu C-C, Vitale S, Roberts C, Miller P, Aryana K, Kang M, et al. Learning from failure: boosting cycling endurance of optical phase change materials. Photonic Phononic Prop Eng Nanostructures XIII. 2023;12431:39–47.

67. Chen C-F, Schrott A, Lee MH, Raoux S, Shih YH, Breitwisch M, et al. Endurance improvement of Ge2Sb2Te5-based phase change memory. IEEE Int Mem Workshop. 2009:1–2.
68. Zhang Y, Chou JB, Li J, Li H, Du Q, Yadav A, et al. Broadband transparent optical phase change materials for high-performance nonvolatile photonics. Nat Commun. 2019;10(1):4279.
69. Castillo SG, Feng Lu, Bachmann T, Bandhu L, Talagrand C, Triggs G, et al. 57-4: Solid state reflective display (SRD®) with LTPS Diode backplane. SID Symp Dig Tech Pap. 2019;50(1):807–10.
70. Taghinejad H, Abdollahramezani S, Eftekhar AA, Fan T, Hosseinnia AH, Hemmatyar O, et al. ITO-based microheaters for reversible multi-stage switching of phase-change materials: towards miniaturized beyond-binary reconfigurable integrated photonics. Opt Express. 2021;29(13):20449–62.
71. Wang S-L, Chen C-Y, Hsieh M-K, Lee W-C, Kung AH, Peng L-H. Phase-change memory devices based on gallium-doped indium oxide. Appl Phys Lett. 2009;94(11):113503.
72. Youngblood N, Talagrand C, Porter B, Galante, CG, Kneepkens S, Sarwat, SG, et al. Broadly-tunable smart glazing using an ultra-thin phase-change material. Appl Phys. 2019.
73. Zhang H, Zhou L, Lu L, Xu J, Wang N, Hu H, et al. Miniature multilevel optical memristive switch using phase change material. ACS Photonics. 2019;6(9):2205–12.
74. Zhang X, Shi G, Leveillee JA, Giustino F, Kioupakis E. Ab initio theory of free-carrier absorption in semiconductors. Phys Rev B. 2022;106(20):205203.
75. Zheng J, Fang Z, Wu C, Zhu S, Xu P, Doylend JK, et al. Nonvolatile electrically reconfigurable integrated photonic switch enabled by a silicon PIN diode heater. Adv Mater. 2020;32(31):2001218.
76. Ríos C, Zhang Y, Shalaginov MY, Deckoff-Jones S, Wang H, An S, et al. Multi-level electro-thermal switching of optical phase-change materials using graphene. Adv Photonics Res. 2021;2(1):2000034.
77. Zhang Y, Ríos C, Shalaginov MY, Li Mo, Majumdar A, Gu T, et al. Myths and truths about optical phase change materials: a perspective. Appl Phys Lett. 2021;118(21):210501.
78. Kim HJ, Sohn J-W, Hong N, Williams C, Humphreys W. PCM-net: a refractive index database of chalcogenide phase change materials for tunable nanophotonic device modelling. J Phys Photonics. 2021;3(2):024008.
79. Lu Y, Stegmaier M, Nukala P, Giambra MA, Ferrari S, Busacca A, et al. Mixed-mode operation of hybrid phase-change nanophotonic circuits. Nano Lett. 2017;17(1):150–55.
80. Farmakidis N, Youngblood N, Lee JS, Feldmann J, Lodi A, Li X, et al. Electronically reconfigurable photonic switches incorporating plasmonic structures and phase change materials. Adv Sci. 2022;9(20):2200383.
81. Cheng Z, Ríos C, Pernice WHP, Wright CD, Bhaskaran H. On-chip photonic synapse. Sci Adv. 2017;3(9):e1700160.
82. Martin-Monier L, Popescu CC, Ranno L, Mills B, Geiger S, Callahan D, et al. Endurance of chalcogenide optical phase change materials: a review. Opt Mater Express. 2022;12(6):2145–67.
83. Teo TYu, Li N, Tobing LYM, Tong ASK, Ng DKT, Ren Z, et al. Capping layer effects on Sb2S3-based reconfigurable photonic devices. ACS Photonics. 2023:3203-14.
84. Shastri BJ, Tait AN, Ferreira De Lima T, Pernice WHP, Bhaskaran H, Wright CD, et al. Photonics for artificial intelligence and neuromorphic computing. Nat Photonics. 2021;15(2):102–14.

How to cite this article: Lee C-Y, Lian C, Sun H, Huang Y-S, Acharjee N, Takeuchi I, et al. Spatial and temporal control of glassy-crystalline domains in optical phase change materials. J Am Ceram Soc. 2024;107:1543–1556.
https://doi.org/10.1111/jace.19541